

Chapter 11

Gaussian Waves and Open Resonators

A large number of gas and solid state lasers as well as free-electron lasers make use of an open resonator.

Before discussing open resonators, we introduce the Gaussian wave (=Gaussian beam). It is a kind of a natural mode of electromagnetic radiation in free space. A Gaussian wave is a paraxial wave, that is a wave with a well-defined propagation direction along the beam axis (z axis) and a small divergence. The amplitude of the field perpendicular to the beam axis has a Gaussian distribution. A Gaussian beam traveling from $z = -\infty$ to $z = \infty$ has a beam waist. Accordingly, the diameter of the beam shows a minimum at the beam waist.

A Gaussian wave is a solution of the wave equation—which we use in the form of the Helmholtz equation—and an appropriate boundary condition: the energy transported by the wave through a plane perpendicular to the propagation direction is finite. Besides the Gaussian mode (=fundamental Gaussian mode), the wave equation provides higher order Gaussian modes.

A Gaussian wave fits to a resonator with spherical mirrors—a longitudinal mode of an open resonator is a standing wave composed of two Gaussian waves propagating in opposite directions. Higher order Gaussian modes lead to transverse modes of a resonator. A laser with a spherical-mirror resonator is able to generate a Gaussian wave.

The analysis of resonators having mirrors of various curvature shows that there are stable and unstable resonators. The confocal, the concentric, and the plane parallel resonator are three special types of resonators.

We describe the effect of diffraction that can be used to suppress laser oscillation on transverse modes and to operate a laser on longitudinal modes only.

We introduce the ray matrix (ABCD matrix) to describe the propagation of paraxial optical rays in free space and in optical systems. We show that a Gaussian beam can be focused by a lens to an area of a diameter that is equal to about a wavelength of the radiation.

The wavelength of a monochromatic Gaussian wave is a constant far outside the beam waist but shows a (small) variation in the range of the waist. As a consequence, the resonance frequencies of a resonator with spherical mirrors are not multiples of a minimum frequency but are shifted toward higher frequencies. The change of wavelength in a beam waist corresponds to a change of phase that has been predicted and experimentally demonstrated by L. G. Gouy in 1891 and experimentally demonstrated also recently by the use of femtosecond pulses. The Gouy phase shift influences the frequency spectrum of optical frequency combs (Sect. 13.4).

We begin this chapter with a characterization of laser radiation generated by the use of a resonator with spherical mirrors.

11.1 Open Resonator

Figure 11.1a shows a design of a laser (e.g., of a titanium-sapphire laser). The laser resonator consists of spherical mirrors (diameter 1 cm) at a distance of 1 m. The active medium has a diameter of 1 cm. The diameter of the laser wave is about 1 mm. The spherical mirrors have the extraordinary property to concentrate the radiation within the resonator at the resonator axis. The radiation circulates within the resonator. A portion of radiation, coupled out via the partial reflector, has a small beam divergence

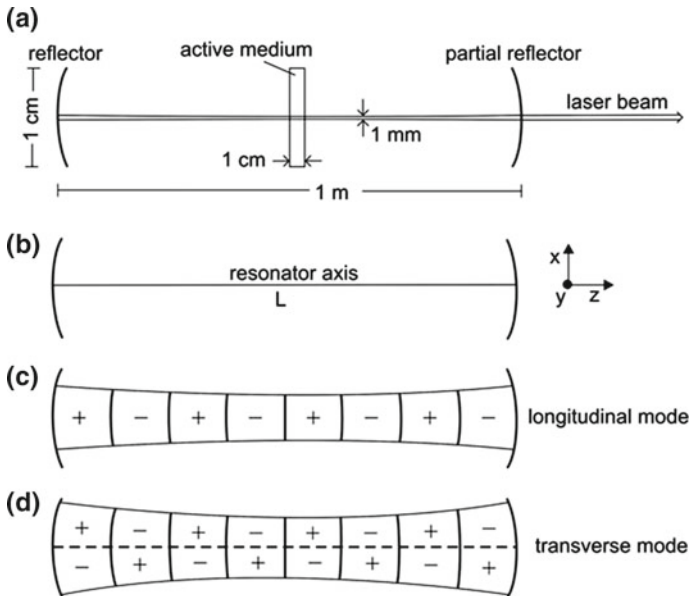


Fig. 11.1 Laser with a spherical-mirror and modes of the resonator. **a** Laser. **b** Open resonator. **c** Longitudinal mode. **d** Transverse mode

(e.g., 1 mrad). Diffraction of the wave at the reflector and the partial mirror has (in the laser design shown in the figure) almost no effect on the wave—except that diffraction plays an important role with respect to elimination of radiation belonging to unwanted modes (Sect. 12.2).

We give here a short characterization of a spherical-mirror resonator: it is an open resonator—it has no sidewalls (Fig. 11.1b). The length L of the resonator is much larger than the wavelength of the radiation. We characterize the modes of the resonator by the use of a cartesian coordinate system; we choose the direction of the resonator axis as z axis. We now blow up the lateral extension of the wave in order to visualize different modes. The simplest type is a *longitudinal mode* (Fig. 11.1c). The phase of the field varies along the resonator axis. The field amplitude has the largest value on the resonator axis and decreases in directions perpendicular to the resonator axis. Figure 11.1d shows a *transverse mode*: the phase of the field varies in axial direction (as for a longitudinal mode); however, the amplitude of the field is zero at the resonator axis and changes the sign in x direction. There are many other types of transverse modes as we will see.

We will show that longitudinal and transverse modes of a resonator with spherical mirrors correspond to standing waves in accord with the wave equation and with appropriate boundary conditions. A standing wave in a spherical-mirror resonator consists of two Gaussian waves propagating in $+z$ and $-z$ direction. The waves are Gaussian waves (=Gaussian beams). Before treating resonators, we will introduce Gaussian waves as solutions of the wave equation describing electromagnetic waves in free space (*see* the next two sections). A Gaussian wave is a paraxial wave: it has a well-defined propagation direction and a small beam divergence. We will see that Gaussian waves in free space can also be divided into longitudinal and transverse modes. A Gaussian (or higher-order Gaussian) mode of the free space is characterized by the propagation direction (z direction) and a number pair mn , where m is the number of changes of the sign of the amplitude in x direction and n is the number of changes in y direction.

The electric field of a Gaussian wave in free space is transverse or nearly transverse to the z direction. The direction of the magnetic field (that has always a direction perpendicular to the electric field) is also transverse or nearly transverse to the z direction. A Gaussian wave characterized as

TEM_{mn} wave

means that the electric and magnetic fields of the wave are transverse or nearly transverse to the z direction (Problem 11.6). A TEM_{mn} wave can be a longitudinal or a transverse mode.

- *Longitudinal mode* = 00 mode = axial mode = Gaussian mode = fundamental Gaussian mode = lowest-order Gaussian mode—the longitudinal mode appears under different names which will become clear during this chapter. The phase of the field in a longitudinal mode varies in the axial (=longitudinal) direction. The sign of the amplitude does not change in the directions perpendicular to the resonator axis.

- *Transverse mode* (=higher-order Gaussian mode). The phase of a transverse mode varies in the axial direction and the sign of the amplitude varies in one or two directions perpendicular to the resonator axis. We will introduce the Hermite–Gaussian modes.

Paraxial electromagnetic waves are transverse electromagnetic (TEM) waves (=transversely polarized electromagnetic waves), whether they belong to longitudinal or transverse modes. The active medium of a laser resonator is able to excite a standing Gaussian mode in the resonator and—if one of the spherical mirrors is a partial mirror—also a Gaussian wave propagating in free space.

A Gaussian mode or a higher-order Gaussian mode within a resonator is a

TEM_{mn l} mode.

The index l indicates the number of half wavelengths of the field in a resonator. The electric and magnetic fields of a Gaussian wave in a resonator are transverse or nearly transverse to the z direction. Each number triple corresponds to a mode of the electromagnetic field, i.e., to a particular pattern of the field in a resonator.

A polarized electromagnetic wave in a mode mn of free space or on a mode $mn $l$$ of a resonator can be polarized in one of two directions perpendicular to each other (and perpendicular to the propagation direction). The direction of the polarization of laser radiation can be chosen by inserting a polarizer or other elements (for instance, a Brewster window) into the laser resonator.

The characterization of modes as longitudinal or transverse modes is of practical interest: most lasers generate radiation belonging mainly to longitudinal modes.

11.2 Helmholtz Equation

We make use of a simple wave optics, first described by Helmholtz. We start with the equation

$$\nabla^2 \mathbf{E} - \frac{1}{c^2} \frac{\partial^2 \mathbf{E}}{\partial t^2} = 0, \quad (11.1)$$

which represents three wave equations, one for each of the three components of the field vector \mathbf{E} . Ignoring the polarization of the electric field, we can reduce the three wave equations to one equation,

$$\nabla^2 E - \frac{1}{c^2} \frac{\partial^2 E}{\partial t^2} = 0. \quad (11.2)$$

E is the field treated as a scalar quantity. We consider a monochromatic wave

$$E(x, y, z, t) = \psi(x, y, z) e^{i\omega t}. \quad (11.3)$$

The time independent part of the field, $\psi(x, y, z)$, obeys the *Helmholtz equation*

$$\nabla^2 \psi + k^2 \psi = 0, \quad (11.4)$$

where $k = \omega/c$. The energy density of the field is $u(x, y, z) = \frac{1}{2} \epsilon_0 |\psi(x, y, z)|^2$. Among the many solutions of the Helmholtz equation are two simple cases.

Plane wave. The solution is

$$E = A e^{i(\omega t - kz)}, \quad (11.5)$$

where

$$k = \omega/c \quad (11.6)$$

is the wave vector and c the speed of light. The wave vector is independent of x , y , and z . The phase of the wave assumes constant values,

$$\varphi(t, z) = \omega t - kz = \text{const.} \quad (11.7)$$

The condition $\partial\varphi/\partial t = 0$ yields the phase velocity $v_{\text{ph}} = dz/dt = \omega/k = c$. The condition $\partial\varphi/\partial z = 0$ yields the group velocity $v_{\text{g}} = dz/dt = c$. Group and phase velocities are equal to the speed of light. The wavelength $\lambda = 2\pi/k$, i.e., the spatial period, is independent of x , y , and z . The amplitude A of a plane wave is the same everywhere in space. The phase kz is a constant in planes of fixed z .

The wave has no angular spread. We can decompose the phase,

$$\varphi(t, z) = \varphi_t(t) - \varphi_z(z), \quad (11.8)$$

where $\varphi_t(t)$ is the time-dependent portion of the phase and $\varphi_z(z)$ is the position-dependent portion. The temporal change of $\varphi_t(t)$ is the angular frequency,

$$d\varphi_t/dt = \omega, \quad (11.9)$$

and spatial change of $\varphi_z(z)$ is the wave vector ($=2\pi \times$ spatial frequency),

$$d\varphi_z/dz = k. \quad (11.10)$$

Spherical wave. A spherical wave has the form

$$E = \frac{K}{s} e^{i(\omega t - ks)}. \quad (11.11)$$

K is a measure of the strength of a wave. Inserting (11.11) in (11.4) yields $k = \omega/c$. The amplitude decreases inversely proportional to the distance s from a point source. The phase ks is a constant on spheres around the origin $s=0$. The phase and group velocities are equal to the speed of light. The direction of the phase and of the group

velocity is radial away from the source point $s = 0$. The wavelength $\lambda = 2\pi/k$ is independent of x , y , and z .

The plane wave and the spherical wave cannot be realized experimentally. We will now look for *paraxial waves*. These have a well-defined propagation direction (along z) and a small angular spread. We describe the waves by the ansatz

$$\psi = f(x, y, z) e^{-ikz}. \quad (11.12)$$

We suppose that f changes only weakly with z . We can therefore neglect the second derivative of f with respect to z and obtain the Helmholtz equation of paraxial waves,

$$\frac{\partial^2 f}{\partial x^2} + \frac{\partial^2 f}{\partial y^2} - 2ik \frac{\partial f}{\partial z} = 0. \quad (11.13)$$

Gaussian waves and waves in optical resonators are described in many textbooks; *see* REFERENCES at the end of the chapter. Studies of mode patterns began in 1961 [67–69]. We will study various aspects of Gaussian waves. We will begin with the discussion of a solution of the Helmholtz equation, following [40].

11.3 Gaussian Wave

A Gaussian wave (=Gaussian beam) is a paraxial wave. We solve the Helmholtz equation of paraxial waves by use of the ansatz

$$f(x, y, z) = G(z) e^{-(x^2+y^2)/F(z)}. \quad (11.14)$$

G and F are complex functions that change only weakly with z .

Differentiation yields

$$\frac{d^2 f}{dx^2} = \left(-\frac{2G}{F} + 4x^2 \frac{G}{F^2} \right) e^{-(x^2+y^2)/F}, \quad (11.15)$$

$$\frac{df}{dz} = \left(\frac{dG}{dz} + \frac{x^2 + y^2}{F^2} G \frac{dF}{dz} \right) e^{-(x^2+y^2)/F}. \quad (11.16)$$

The Helmholtz equation leads to an equation

$$-\frac{2}{F(z)} - ik \frac{1}{G(z)} \frac{dG(z)}{dz} + \frac{x^2 + y^2}{F^2(z)} \left(2 - ik \frac{dF}{dz} \right) = 0, \quad (11.17)$$

which includes two conditions,

$$2 - ik \frac{dF}{dz} = 0, \quad (11.18)$$

$$-\frac{2}{ikF} - \frac{1}{G} \frac{dG}{dz} = 0. \quad (11.19)$$

Integrating (11.18) yields

$$F(z) = \frac{2}{ik}(z + C_1). \quad (11.20)$$

The integration constant C_1 is a complex quantity. We suppose that the wave front at $z = z_0$ is a plane, i.e., that the phase of $f(x, y, z)$ is independent of x and y . Then $F(z_0)$ is real. By writing $F(z_0) = w_0^2$, we find

$$C_1 = \frac{ik}{2}w_0^2 - z_0 \quad (11.21)$$

and

$$F = w_0^2 + \frac{2}{ik}(z - z_0). \quad (11.22)$$

We separate $1/F$ in real and imaginary part,

$$\frac{1}{F} = \frac{k^2 w_0^2 + 2ik(z - z_0)}{k^2 w_0^4 + 4(z - z_0)^2} = \frac{1}{w^2} + \frac{ik}{2R}, \quad (11.23)$$

where

$$w = w_0 \sqrt{1 + \frac{4(z - z_0)^2}{k^2 w_0^4}}, \quad (11.24)$$

$$R = z - z_0 + \frac{k^2 w_0^4}{4(z - z_0)}. \quad (11.25)$$

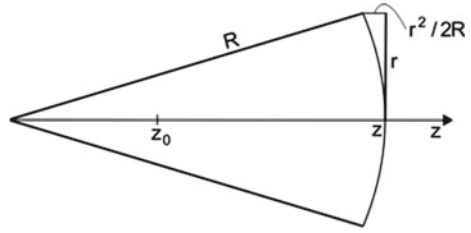
We obtain, with $r^2 = x^2 + y^2$, the solution

$$f(z, r) = G(z) e^{-r^2/w^2(z)} e^{-ikr^2/2R(z)}. \quad (11.26)$$

We will see that $w = w(z)$ is the beam radius and $R = R(z)$ is the radius of curvature of the beam at the location z . The beam radius has the smallest value for $z = z_0$, i.e., the beam has a waist at $z = z_0$, where the radius of the beam is equal to w_0 . That R is the radius of curvature follows from the relation (Fig. 11.2):

$$\frac{2(z - z_0)r^2}{k^2 w_0^4 + 4(z - z_0)^2} = \frac{r^2}{2R}. \quad (11.27)$$

Fig. 11.2 Curvature of the wave front of a Gaussian wave



Making use of (11.22) and (11.19) we obtain the differential equation

$$\frac{1}{G} \frac{dG}{dz} = -\frac{1}{z - z_0 + ikw_0^2/2}. \quad (11.28)$$

We write

$$G(z) = K(z) e^{i\phi(z)}. \quad (11.29)$$

$K=|G|$ is the absolute value of G and ϕ is a phase, the *Gouy phase*. We obtain the differential equation

$$\frac{1}{G} \frac{dG}{dz} = \frac{1}{K} \frac{dK}{dz} + i \frac{d\phi}{dz} = -\frac{z - z_0}{(z - z_0)^2 + k^2 w_0^4/4} + \frac{ikw_0^2/2}{(z - z_0)^2 + k^2 w_0^4/4}. \quad (11.30)$$

Separation of real and imaginary part provides two differential equations,

$$\frac{1}{K} \frac{dK}{dz} = \frac{z - z_0}{(z - z_0)^2 + k^2 w_0^4/4}, \quad (11.31)$$

$$\frac{d\phi}{dz} = \frac{k w_0^2/2}{(z - z_0)^2 + k^2 w_0^4/4}. \quad (11.32)$$

The solutions are

$$K = \frac{2C_2}{k w_0^2}, \quad (11.33)$$

$$\phi(z) = \tan^{-1} \frac{2(z - z_0)}{k w_0^2} \quad \text{or} \quad \tan \phi(z) = \frac{2(z - z_0)}{k w_0^2}. \quad (11.34)$$

C_2 is an integration constant, which is real. (Instead of the notation \tan^{-1} , the notation \arctan can be used). It follows that the field is

$$\psi(z, r) = \frac{C_3}{w(z)} e^{-r^2/w^2(z)} e^{-i[kz - \phi(z) + kr^2/2R(z)]}. \quad (11.35)$$

$C_3 = 2C_2/kw_0$ is a constant. The phase shows a change according to propagation and, additionally, due to the Gouy phase shift $\phi(z)$. The amplitude of the field decreases in propagation direction inversely proportional to the beam radius. The field amplitude at a fixed z decreases from its value on the axis ($r = 0$) to $1/e$ at the beam radius $w(z)$. The solution contains two integration constants, w_0 (contained in the expression of w) and C_3 . The values of w_0 and C_3 of a particular Gaussian wave can be determined experimentally—for instance by determination of the beam diameter of the intensity distribution at a fixed location z (e.g., at z_0) and determination of the power of the wave. In the *beam waist*, i.e., at the location of minimum beam diameter, the field distribution is equal to

$$\psi(z_0, r) = \frac{C_3}{w_0} e^{-r^2/w_0^2} e^{-i[kz_0 - \phi(z_0)]}. \quad (11.36)$$

We can write

$$G(z) = \frac{C_2}{z + C_1} = \frac{C_2}{ikF(z)/2} \quad (11.37)$$

and therefore

$$\psi(z, r) = \frac{2C_2}{ikF(z)} e^{-r^2/w^2(z)} e^{-i[kz - \phi(z) + kr^2/2R(z)]}, \quad (11.38)$$

where

$$\frac{1}{F(z)} = \frac{1}{w^2(z)} + \frac{ik}{2R(z)}. \quad (11.39)$$

The propagation of a Gaussian wave is completely described by the beam radius $w(z)$ and the radius of curvature $R(z)$ or, alternatively, by the complex beam parameter $F(z)$. It is convenient to introduce another complex beam parameter

$$\tilde{q}(z) = \frac{ik}{2} F(z). \quad (11.40)$$

(We omit in this section the tilde sign of complex quantities, except of the beam parameter \tilde{q}). It follows that

$$\frac{1}{\tilde{q}(z)} = \frac{1}{R(z)} - \frac{2i}{kw^2(z)} = \frac{1}{R(z)} - \frac{i\lambda}{\pi w^2(z)}. \quad (11.41)$$

We can write the field in the form

$$\psi(z, r) = \frac{2C_2}{ikF} \exp\left(-ikz - \frac{r^2}{F}\right) = \frac{C_2}{\tilde{q}} \exp\left(-ikz - \frac{r^2}{2\tilde{q}}\right). \quad (11.42)$$

We now discuss the solution in more detail. The field is equal to

$$E(z, r) = \frac{C_3}{w(z)} e^{-r^2/w^2(z)} e^{i(\omega t - [kz - \phi(z) + kr^2/2R])}. \tag{11.43}$$

The spatially dependent part is

$$\psi(z, r) = \frac{C_3}{w(z)} e^{-r^2/w^2(z)} e^{-i[kz - \phi(z) + kr^2/2R]}. \tag{11.44}$$

We write

$$\psi(z, r) = A(z, r) e^{-i\varphi(z, r)}. \tag{11.45}$$

The amplitude of the Gaussian wave is

$$A(z, r) = \frac{C_3}{w(z)} e^{-r^2/w^2(z)} \tag{11.46}$$

and the phase is

$$\varphi(z, r) = kz - \phi(z) + \frac{r}{2R(z)} kr. \tag{11.47}$$

The expression contains two terms that depend on z only and another term that depends additionally on r ; this term vanishes on the beam axis. The field distribution has the following properties (Fig. 11.3 and Table 11.1):

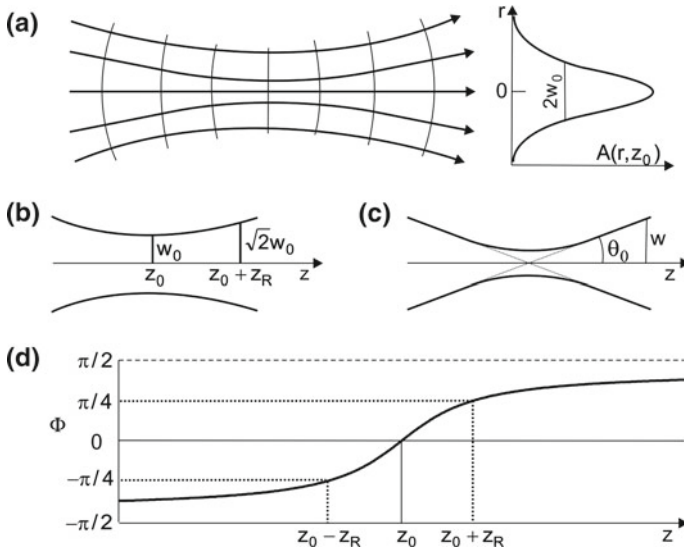


Fig. 11.3 Gaussian wave. **a** Rays and lateral distribution of the amplitude. **b** Rayleigh range. **c** Divergence. **d** Gouy phase

Table 11.1 Properties of field and energy density of a Gaussian beam propagating from $z = -\infty$ to $z = +\infty$

	$z = -\infty$	$z = z_0$	$z = (z_0 + z_R)$	$z \rightarrow \infty$
Radius (field)		w_0	$\sqrt{2} w_0$	$w_0(z - z_0)/z_R$
$A(r = 0)$		A_0	$A_0/\sqrt{2}$	$A_0 z_R/(z - z_0)$
ϕ	$-\pi/2$	0	$\pi/4$	$\pi/2$
Wave front	Spherical	Plane	Curved	Spherical
Radius (energy)		$r_{u,0} = w_0/\sqrt{2}$	$\sqrt{2} r_{u,0}$	$r_{u,0}(z - z_0)/z_R$
$u(r=0)$	$u_0 z_0^2/(z - z_0)^2$	u_0	$u_0/2$	$u_0 z_0^2/(z - z_0)^2$

- $\psi(r, z)$ is circularly symmetric around the beam axis.
- The amplitude of the wave decreases laterally according to the Gaussian function and is, on the beam axis, inversely proportional to the beam radius $w(z)$.
- The wave has a waist. The beam radius of the waist is w_0 . In the waist, the wave front is a plane and the field amplitude distribution is given by

$$A(z_0, r) = \frac{C_3}{w_0} e^{-r^2/w_0^2} = A_0 e^{-r^2/w_0^2}. \tag{11.48}$$

A_0 is the amplitude of the wave on the beam axis ($r=0$) at $z=z_0$.

- If $z \neq z_0$, the wave front is curved and the beam radius increases with increasing $|z - z_0|$.
- For large $|z - z_0|$, namely for $|z - z_0| \gg kw_0^2/2$, the curvature is $R(z) = z - z_0$ and the beam radius is $w(z) = 2kw_0(z - z_0)$. Both the curvature and the beam radius increase linearly with $|z - z_0|$.
- The *Rayleigh range* is equal to

$$z_R = kw_0^2/2 = \pi w_0^2/\lambda. \tag{11.49}$$

The beam diameter increases in the range $z_0, z_0 + z_R$ by the factor $\sqrt{2}$. In the range $z_0 - z_R, z_0 + z_R$ the Gaussian wave remains almost parallel. This range is the near-field (or Fresnel) range. The range $|z - z_0| > z_R$ is the far-field (Fraunhofer) range. We can express the three parameters w, R , and ϕ of a Gaussian wave by the beam waist w_0 and the Rayleigh range z_R ,

$$w(z) = w_0 \sqrt{1 + \frac{(z - z_0)^2}{z_R^2}}, \tag{11.50}$$

$$R(z) = z - z_0 + \frac{z_R^2}{z - z_0}, \tag{11.51}$$

$$\phi(z) = \tan^{-1} \frac{z - z_0}{z_R}. \tag{11.52}$$

The distance $2z_R$ between the points $z_0 - z_R$ and $z_0 + z_R$ is the *confocal parameter* or *depth of focus*.

- *Gouy phase*. The Gouy phase—inherent to a Gaussian wave—describes a phase that is associated with the spatial and the temporal change of the curvature of the wave front (Sect. 11.7).
- *Change of phase*. When a wave front with the field distribution $\psi(z_1, r)$ propagates from z_1 to z_2 , the phase φ changes according to

$$\varphi(z_2) - \varphi(z_1) = [kz_2 - \phi(z_2)] - [kz_1 - \phi(z_1)]. \quad (11.53)$$

$\varphi(z_2) - \varphi(z_1)$ is the Gouy phase shift. When the wave front propagates through the beam waist from a far-field location $z_1 \ll z_0$ to a far-field location $z_2 \gg z_0$, the phase φ changes by

$$\varphi(z_2) - \varphi(z_1) = kz_2 - kz_1 - \pi. \quad (11.54)$$

The propagation through the beam waist changes the phase of the wave by $-\pi$, in addition to the geometrical phase change $kz_2 - kz_1$. When the wave front travels from $z_1 = -z_R$ to $z_2 = z_R$, the change of phase is (for $z_0 = 0$) equal to

$$\varphi(z_R) - \varphi(-z_R) = kz_R - \pi/2. \quad (11.55)$$

- The field of a Gaussian wave is given by

$$E(z, r, t) = A_0 \frac{w_0}{w} e^{-r^2/w^2(z)} \cos[\omega t - (kz - \phi + kr^2/2R)]. \quad (11.56)$$

$A_0 = C_3/w_0$ is the amplitude in the center of the beam waist (at $z = 0$ and $r = 0$).

- The energy density, averaged over a temporal period, is

$$u(z, r) = \frac{1}{2} \varepsilon_0 A_0^2 \frac{r_{u,0}^2}{r_u^2} e^{-r^2/r_u^2}, \quad (11.57)$$

where $r_u = w/\sqrt{2}$ is the beam radius with respect to the energy density distribution. The radius of the energy distribution at the beam waist is $r_{u,0} = w_0/\sqrt{2}$. At the beam waist, the energy density decreases within the radius $r_{u,0}$ to $1/e$ relative to the energy density on the beam axis.

- *Divergence*. At large $|z - z_0|$, the angle of divergence of the field is given by

$$\theta_0 = \frac{w_0}{z_R} = \frac{\lambda}{\pi w_0}. \quad (11.58)$$

The product of the far-field aperture angle θ_0 and the diameter at the beam waist is a constant,

$$2w_0 \times \theta_0 = 2\lambda/\pi. \quad (11.59)$$

The angle of divergence, with respect to the energy density, is $\theta_{u,0} = \theta_0/\sqrt{2}$. The product

$$2r_{u,0}\theta_{u,0} = \lambda/\pi \quad (11.60)$$

is by a factor of two smaller than the product with respect to the field amplitude.

- *Radiance of a Gaussian wave.* The radiance of a paraxial beam is defined as the power of radiation passing through an area (oriented perpendicular to the beam direction) divided by the area and the solid angle of the beam. To estimate the radiance of a Gaussian beam, we approximate $\exp(-r^2/r_u^2)$ by a rectangular radial distribution of diameter $2r_u$ and find that the power of radiation passing through the beam waist is approximately given by

$$P = L_u \times \text{area} \times \Omega, \quad (11.61)$$

which is the product of the area of the beam in the beam waist, the solid angle Ω of the beam, and the radiance (=brightness) L_u . We can write:

$$L_u = \frac{P}{\text{area} \times \Omega}. \quad (11.62)$$

For small values of $\theta_{u,0}$, the solid angle of the beam is $\Omega = \pi\theta_{u,0}^2$. This leads to

$$L_u = \frac{P}{\pi r_{u,0}^2 \times \pi \theta_{u,0}^2}. \quad (11.63)$$

Taking into account the relation (11.60), we find that the radiance of a Gaussian beam is equal to the power divided by $(\lambda/2)^2$.

Example $P=1$ W; $\lambda=0.5$ μm ; $L_u=1.6 \times 10^{13}$ $\text{W m}^{-2} \text{sr}^{-1}$.

Is it possible to realize a Gaussian wave? The answer is: a laser with appropriately arranged spherical mirrors as resonator mirrors is able to produce a Gaussian wave. We will begin the discussion of spherical-mirror resonators by treating a particular spherical-mirror resonator, the symmetric confocal resonator.

11.4 Confocal Resonator

A confocal resonator consists of two spherical mirrors, which have the same focus. We discuss the symmetric confocal resonator. It has two equal mirrors.

Two spherical mirrors arranged at a distance $L=R$ form a (symmetric) *confocal resonator* (Fig. 11.4, left). We choose $z=0$ as the location of the center of one of the mirrors. We will show that a Gaussian wave can fit to a confocal resonator. The symmetry of the arrangement requires that the beam waist lies at $z_0 = L/2$. We choose $z_R = L/2$ and obtain, by using (11.49) and (11.50), the radius of curvature

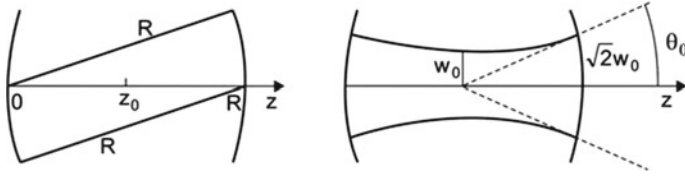


Fig. 11.4 Confocal resonator

$$R = \frac{L}{2} \left(1 + \frac{k^2 w_0^4}{L^2} \right) \quad (11.64)$$

and the beam radius (=mode radius) with respect to the field amplitude in the waist

$$w_0 = \sqrt{\frac{L\lambda}{2\pi}}. \quad (11.65)$$

With respect to the energy density, the mode radius in the beam waist is $r_{u,0} = \sqrt{L\lambda/4\pi}$.

The Gaussian mode within the resonator (Fig. 11.4, right) has the beam waist w_0 . The beam radius on each of the mirrors is $w_0\sqrt{2}$. The distance between the center of the resonator and a mirror is equal to the Rayleigh range. In the far-field range, outside the resonator—with one of the spherical mirrors being a partial reflector—the field has the divergence angle $\theta_0 = 2\lambda/(\pi w_0)$.

The field in the resonator corresponds to a Gaussian standing wave, i.e., to two Gaussian waves propagating in opposite directions,

$$E(z, r) = \frac{1}{2} A(z, r) e^{i[\omega t - \varphi(z, r) + \varphi_0]} + \frac{1}{2} A(z, r) e^{i[\omega t + \varphi(z, r) - \varphi_0]}. \quad (11.66)$$

The field at the axis is equal to

$$E = A_0 \frac{w_0}{w} e^{-r^2/w^2} \cos[kz - \phi(z) - \varphi_0] \cos \omega t. \quad (11.67)$$

We obtain the resonance frequencies by the use of the resonance condition (2.80), namely that the change of the phase of a field propagating in the resonator is, at a round trip transit, a multiple of 2π (that is the resonator eigenvalue problem). The Gouy phase shift per round trip transit is

$$\Delta\phi = \phi(z_2) - \phi(z_1) + \phi(z_2) - \phi(z_1) = 2(\phi(z_2) - \phi(z_1)) = \pi \quad (11.68)$$

This leads to the condition

$$2kL - \Delta\phi = 2kL - \pi = l \times 2\pi \quad (11.69)$$

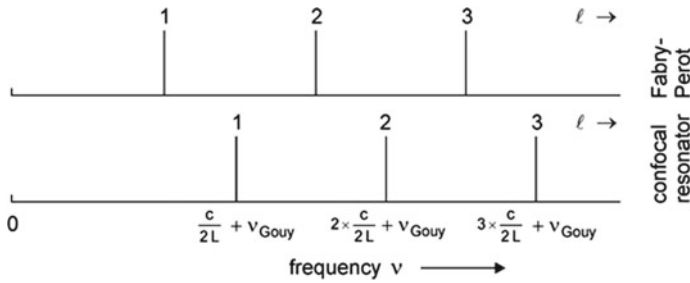


Fig. 11.5 Resonance frequencies

or

$$k_l L = \left(l + \frac{1}{2} \right) \pi; \quad l = 1, 2, \dots \tag{11.70}$$

The resonance frequencies are (Fig. 11.5)

$$\nu_l = \frac{c}{2L} \left(l + \frac{1}{2} \right) = l \times \frac{c}{2L} + \nu_{\text{Gouy}}, \tag{11.71}$$

where $\nu_{\text{Gouy}} = c/4L$ is the Gouy frequency shift for the symmetric confocal resonator. In comparison with a Fabry–Perot interferometer of the same length, the resonance frequencies are shifted towards higher frequencies. However, the frequency separation between adjacent modes is the same,

$$\nu_{l+1} - \nu_l = \frac{c}{2L}. \tag{11.72}$$

The phase φ_0 is determined by the choice of the origin ($z=0$) of the z axis. We have chosen the position of one of the reflectors as $z = 0$. The boundary conditions, namely that the field on the mirror (assumed to have a reflectivity near 1), has to be zero, requires that

$$\varphi_0 + \phi(0) = \varphi_0 - \pi/4 = 3\pi/4 \tag{11.73}$$

and therefore $\varphi_0 = \pi/2$. Thus, we obtain the field at the axis:

$$\psi = A_0 \frac{w_0}{w} e^{-r^2/w^2} \sin[kz - \phi(z)] \cos \omega t. \tag{11.74}$$

The energy density, averaged over both a temporal period and a spatial period, is

$$u = \frac{\epsilon_0}{4} A_0^2 \frac{r_{u,0}^2}{r_u^2} e^{-r^2/r_u^2} = u_0 \frac{r_{u,0}^2}{r_u^2} e^{-r^2/r_u^2}, \tag{11.75}$$

Table 11.2 Beam waist and mode volume of confocal resonators of different lengths suitable for radiation of wavelength $\lambda=0.6 \mu\text{m}$

$L(\text{m})$	$r_{u,0} = \sqrt{L\lambda/4\pi}$	$V_{00} (\text{m}^3)$
0.1	69 μm	1.5×10^{-8}
0.5	155 μm	3.5×10^{-8}
10	0.69 mm	1.5×10^{-5}

where $u_0 = (\varepsilon_0/4)A_0^2$ is the energy density at $r=0$ at the beam waist ($z=z_0$).

The energy contained in a mode is given by

$$\int_0^L dz \int_0^\infty u(r) \times 2\pi r dr = u_0 \int_0^L dz \frac{r_{u,0}^2}{r_u^2} \int_0^\infty 2\pi r dr e^{-r^2/r_u^2} = u_0 \pi r_{u,0}^2 L. \quad (11.76)$$

What is the volume V_0 of a (hypothetical) mode, which contains the same radiation energy as the 00 mode, but with a constant energy density? We can write $u_0 V_{00} = u_0 \pi r_{u,0}^2 L$ and interpret V_{00} as the *mode volume*. Thus, the mode volume of the 00 mode of a confocal resonator is equal to

$$V_{00} = \pi r_{u,0}^2 L. \quad (11.77)$$

The mode volume of the 00 mode of a confocal resonator is equal to the product of the cross sectional area of the beam waist (with respect to the energy distribution) and the length of the resonator. Table 11.2 shows values of beam waists and mode volumes for radiation of a fixed wavelength.

The confocal resonator is suitable as resonator of, for instance, a helium–neon laser or a free-electron laser.

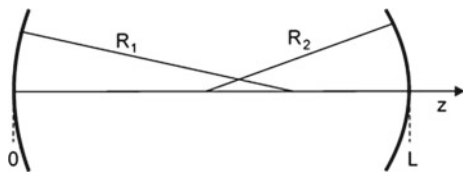
- *Helium–neon laser* ($\lambda=633 \text{ nm}$). The small gain of the active medium requires a large length (typically 0.5 m) of the resonator. The mechanism of the relaxation of the excited neon atoms makes it necessary to use a tube with a small diameter; the neon atoms relax by collisions with the walls (Sect. 14.3).
- *Free-electron laser*. A free-electron laser requires a resonator of a length of typically 10 m. The Gaussian wave in a confocal resonator has a large overlap with an electron wave that propagates along the axis of the resonator (Sect. 19.1).

Other resonator configurations will be discussed in the next section.

11.5 Stability of a Field in a Resonator

There are a large number of different resonators. However, not all have stable modes. We treat a resonator with two spherical mirrors (Fig. 11.6) that have different radii (R_1 and R_2) of curvature. A Gaussian mode, fitting to the resonator, can be determined

Fig. 11.6 Resonators with spherical mirrors



by means of the conditions for the radii of curvature:

$$R_1 = z_0 \left(1 + \frac{z_R^2}{z_0^2} \right) = -R_1(0), \quad (11.78)$$

$$R_2 = (L - z_0) \left(1 + \frac{z_R^2}{(L - z_0)^2} \right), \quad (11.79)$$

where z_0 is the location of the beam waist; $z=0$ and $z=L$ are the positions of the two mirrors. From the two relations, we find

$$z_0 = \frac{(1 - g_1)g_2 L}{g_1 + g_2 - 2g_1 g_2}, \quad (11.80)$$

$$z_R^2 = \frac{(1 - g_1 g_2)g_1 g_2 L^2}{(g_1 + g_2 - 2g_1 g_2)^2}, \quad (11.81)$$

$$w_0^2 = \frac{L\lambda}{\pi} \frac{\sqrt{(1 - g_1 g_2)g_1 g_2}}{g_1 + g_2 - 2g_1 g_2}, \quad (11.82)$$

$$w_i^2 = \frac{L\lambda}{\pi g_i} \sqrt{\frac{g_1 g_2}{1 - g_1 g_2}}, \quad (11.83)$$

where w_i ($i=1, 2$) is the beam radius at the mirror 1 or 2, respectively, and where

$$g_1 = 1 - L/R_1, \quad (11.84)$$

$$g_2 = 1 - L/R_2 \quad (11.85)$$

are the *mirror parameters*. The mode diameters w_i are infinitely large if the product $g_1 g_2 = 1$. There is no real solution if $g_1 g_2 (1 - g_1 g_2)^{-1}$ is negative. This leads to the *stability criterion*: a stable mode can be realized if

$$0 \leq g_1 g_2 \leq 1. \quad (11.86)$$

Fig. 11.7 shows the resonator stability diagram. Stable resonators have mirror parameters in the shadowed regions.

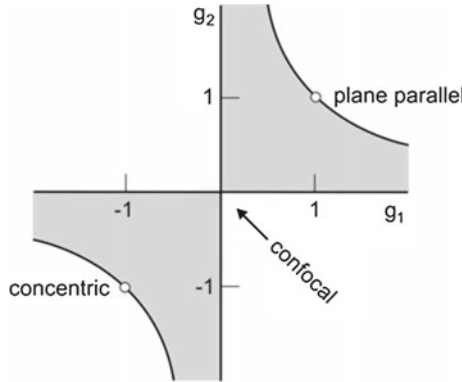


Fig. 11.7 Resonator stability diagram

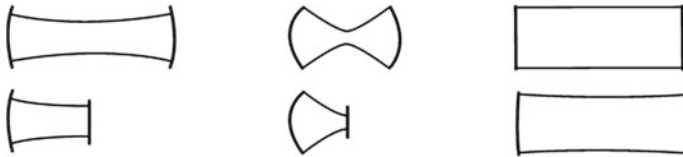


Fig. 11.8 Types of resonators; confocal and semiconfocal (left); near-concentric and semiconcentric (center); planar and near-planar (right)

There are limiting cases.

- $R_1 = R_2 = \infty$; $g_1 = g_2 = 1$; plane parallel (=Fabry-Perot) resonator.
- $R_1 + R_2 = 2L$; $g_1 + g_2 - g_1g_2 = 0$; confocal resonator (general case).
- $R_1 = R_2 = L$; $g_1 = g_2 = 0$; symmetric confocal resonator.
- $R_1 + R_2 = L$; $g_1g_2 = 1$; concentric resonator (general case).
- $R_1 + R_2 = L$; $g_1 = g_2 = -1$; symmetric concentric resonator.

The different types of resonators (Fig. 11.8) have advantages and disadvantages.

- The *confocal resonator*. It has the lowest diffraction loss (Sect. 11.8). Corresponding to the stability criterion, the confocal resonator is at the limit of stability. To reach stability, the distance between the mirrors should be slightly smaller than the radius of curvature of the mirrors. In comparison with other resonators, this resonator can easily be adjusted.
- A *semiconfocal resonator* consists of a spherical mirror and a plane mirror at the distance $R/2$, where R is the radius of curvature of the spherical mirror—the plane mirror is located at the position of the beam waist of a corresponding confocal resonator.
- The *concentric resonator* (=spherical resonator) has a beam waist of $w_0 = 0$ and an infinitely large divergence. It is therefore not realizable.
- The *near-concentric resonator* has the smallest mode volume.

- A *semiconcentric resonator* (=hemispheric resonator) consists of a spherical mirror and a plane mirror at the distance $R/4$ —the plane mirror is located at the position of the beam waist of a corresponding confocal resonator.
- The *plane parallel* (=Fabry-Perot) resonator has, in comparison with all other resonators, the largest mode volume. It is difficult to adjust.
- The *near-planar resonator* (=superconfocal resonator) has one or two mirrors with a radius of curvature that is much larger than the length of the resonator. This resonator has the advantage, in comparison with the plane parallel resonator, that it is easier to adjust. In comparison with the confocal resonator, the near-planar resonator has a larger mode volume at the same resonator length. In special cases, larger laser output power is obtainable. The beam radius of a near-planar resonator, with $R_1=R_2=R \geq L$, is almost constant along the resonator axis,

$$w_0^2 = w_1^2 = w_2^2 = \frac{\lambda L}{\pi} \sqrt{\frac{R}{2L}}. \quad (11.87)$$

The change of the phase of a Gaussian wave propagating in a near-planar resonator during a single transit through a resonator is small, since $\phi(z=0) \approx \phi(z_0) \approx \phi(z=L) \sim 0$. This follows from the expression $\phi = \tan^{-1}(z - z_0)/z_R$.

In the general case of a stable resonator, the change of the Gouy phase shift per round trip transit is given by

$$\Delta\phi = 2[\phi(L) - \phi(0)] = 2 \left(\tan^{-1} \frac{L - z_0}{z_R^2} - \tan^{-1} \frac{-z_0}{z_R^2} \right) = 2 \cos^{-1}(\pm\sqrt{g_1 g_2}). \quad (11.88)$$

We made use of the relations $\tan^{-1} x + \tan^{-1} y = \tan^{-1}([x + y]/[1 - xy])$ and $\tan^{-1} x = \cos^{-1}(1/\sqrt{1 + x^2})$. (Note that the inverse trigonometric function $\cos^{-1} x \equiv \arccos x$.) The condition

$$2kL - \Delta\phi = l \times 2\pi, \quad l = 1, 2, \dots \quad (11.89)$$

leads to the resonance frequencies

$$\nu_l = \frac{c}{2L} \left[l + \frac{1}{\pi} \cos^{-1}(\pm\sqrt{g_1 g_2}) \right], \quad (11.90)$$

where the plus sign has to be chosen if g_1 and g_2 are positive while the minus sign has to be chosen if g_1 and g_2 are negative. Limiting cases are as follows:

- Fabry-Perot resonator. $g_1, g_2 \rightarrow 1$; $\cos^{-1} \sqrt{g_1 g_2} \rightarrow 0$.
- Confocal resonator; $g_1, g_2 \rightarrow 0$; $\cos^{-1} \sqrt{g_1 g_2} \rightarrow \pi/2$.
- Concentric resonator; $g_1, g_2 \rightarrow -1$; $\cos^{-1} \sqrt{\pm g_1 g_2} \rightarrow \pi$.

The frequency difference between adjacent modes is

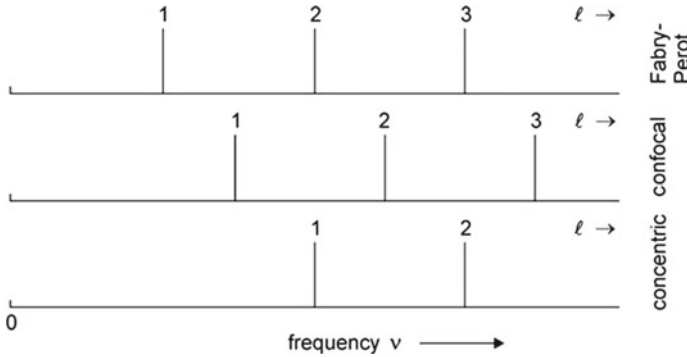


Fig. 11.9 Resonance frequencies of different resonators

$$\nu_{l+1} - \nu_l = c/(2L). \tag{11.91}$$

This is an important result: the Gouy phase shift of radiation propagating within a resonator causes a shift of the resonance frequencies of the resonator toward higher frequencies. The shift is the same for all resonance frequencies. But the frequency distance between neighboring resonances remains uninfluenced by the Gouy phase shift.

Figure 11.9 shows the frequencies of the modes of different resonators. The Gouy frequency is zero for a Fabry-Perot resonator, $c/4L$ for a symmetric confocal resonator, and $c/2L$ for a symmetric concentric resonator.

11.6 Transverse Modes

We use the ansatz

$$f(x, y, z) = X(x) Y(y) G(z) e^{-(x^2+y^2)/F(z)}, \tag{11.92}$$

where X depends on x only, Y on y only, F and G on z only. Differentiation yields

$$\frac{\partial^2 f}{\partial x^2} = \left(X'' - \frac{4x}{F} X' - \frac{2}{F} X + \frac{4x^2}{F^2} \right) XYGe^{-r^2/F}, \tag{11.93}$$

$$\frac{\partial f}{\partial z} = \left[G' + \frac{GF'}{F^2} (x^2 + y^2) \right] XYe^{-r^2/F}, \tag{11.94}$$

with $X' = dX/dx$, $Y' = dY/dy$ and $G' = dG/dz$. The Helmholtz differential equation leads to

$$\frac{X''}{X} - \frac{4x}{F} \frac{X'}{X} + \frac{Y''}{Y} - \frac{4y}{F} \frac{Y'}{Y} - \frac{4}{F} - 2ik \frac{G'}{G} + 2 \frac{x^2 + y^2}{F^2} (2 - ikF') = 0. \tag{11.95}$$

We obtain again the condition that $2 - ikF' = 0$. With the same arguments used earlier, we find again that $F(z) = w_0^2 + 2/(ik)(z - z_0)$. Furthermore, we obtain differential equations for X and Y ,

$$\frac{X''}{X} - \frac{4x}{F} \frac{X'}{X} + \frac{4m}{F} = 0, \quad (11.96)$$

$$\frac{Y''}{Y} - \frac{4y}{F} \frac{Y'}{Y} + \frac{4n}{F} = 0, \quad (11.97)$$

where m and n are dimensionless numbers. We introduce the dimensionless variable $\zeta = x\sqrt{2/F}$. Then the differential equation for X becomes

$$\frac{d^2 X}{d\zeta^2} - 2\zeta \frac{dX}{d\zeta} + 2mX = 0. \quad (11.98)$$

This is Hermite's differential equation. The solutions are the Hermite polynomials $H_m(\zeta)$; H_m is the Hermite polynomial of m th order. We list a few Hermite polynomials.

- $m = 0$; $H_0(\zeta) = 1$.
- $m = 1$; $H_1(\zeta) = 2\zeta$.
- $m = 2$; $H_2(\zeta) = 4\zeta^2 - 2$.
- $m = 3$; $H_3(\zeta) = 8\zeta^3 - 12\zeta$.

The Hermite function H_0 is an even function with respect ζ , H_1 is an odd function, H_2 an even function and so on. The Hermite polynomials obey the recursion formula

$$H_{m+1}(\zeta) = 2\zeta H_m(\zeta) - 2m H_{m-1}(\zeta). \quad (11.99)$$

The solutions of (11.96) and (11.97) are

$$X(x) = H_m\left(\sqrt{\frac{2}{F}}x\right) \quad \text{and} \quad Y(y) = H_n\left(\sqrt{\frac{2}{F}}y\right). \quad (11.100)$$

We obtain from (11.95) by separation of the variables the differential equation

$$\frac{G'}{G} = \frac{2i}{k} \frac{1+m+n}{F} = -\frac{1+m+n}{z+C_1}. \quad (11.101)$$

We write

$$G_{mn}(z) = |G_{mn}(z)| e^{i\phi_{mn}(z)}. \quad (11.102)$$

Separation in real and imaginary part leads to two differential equations for $|G|$ and ϕ . The solution for $|G|$ is

$$|G(z)| = |G_{mn}(z)| = \frac{C_{3,mn}}{w}, \quad (11.103)$$

where

$$C_{3,mn} = \frac{C_2}{(kw_0/2)^{1+m+n}} \quad (11.104)$$

and where C_2 is an integration constant, which is real. The solution for ϕ is

$$\phi_{mn}(z) = (1 + m + n) \phi(z). \quad (11.105)$$

$\phi(z)$ is the same as in the case $m = n = 0$. Thus, we have the solution

$$\psi_{mn}(x, y, z) = H_m\left(\sqrt{\frac{2}{F}}x\right) H_n\left(\sqrt{\frac{2}{F}}y\right) \frac{C_{3,mn}}{w(z)} e^{-i(kz - \phi_{mn} + kr^2/2R)}. \quad (11.106)$$

The Gouy phase increases with increasing m and increasing n . Each number pair mn corresponds to a mode of radiation in free space. We design the paraxial modes with $mn=00$ (=fundamental Gaussian modes = Gaussian modes) as *longitudinal modes* and the paraxial modes with $mn \neq 00$ as *transverse modes* (=Hermite-Gaussian modes = higher-order Gaussian modes).

Figure 11.10a shows the amplitudes of the fields of a few modes together with field lines. The amplitudes of longitudinal and transverse modes have different spatial distributions.

- 00 mode. The field amplitude ψ has the largest value at the beam axis.
- 10 mode. In x direction, the amplitude changes once the sign and has two extrema—according to the Hermite polynomial $H_1(x)$. The field amplitude is zero at the beam axis.
- 20 mode. In x direction, the amplitude changes twice the sign and has three extrema.

The transverse modes mnl have the same beam diameter and the same radius of curvature as the longitudinal mode 001. A transverse mnl mode has, along the z axis, the same number of field maxima as the longitudinal 001 mode (compare with Fig. 11.1c and d). Figure 11.10b shows different mode patterns as they can be observed for the intensity distribution of laser radiation outside a laser resonator; special filters placed in a laser resonator can select a particular mode at which a laser oscillates.

The phase shift per round trip transit of radiation in a mode mnl has to obey the resonator eigenvalue condition

$$2kL - (1 + m + n)\Delta\phi = l \times 2\pi, \quad (11.107)$$

where

$$\Delta\phi = \phi(z_2) - \phi(z_1) + \phi(z_2) - \phi(z_1) = 2(\phi(z_2) - \phi(z_1)), \quad (11.108)$$

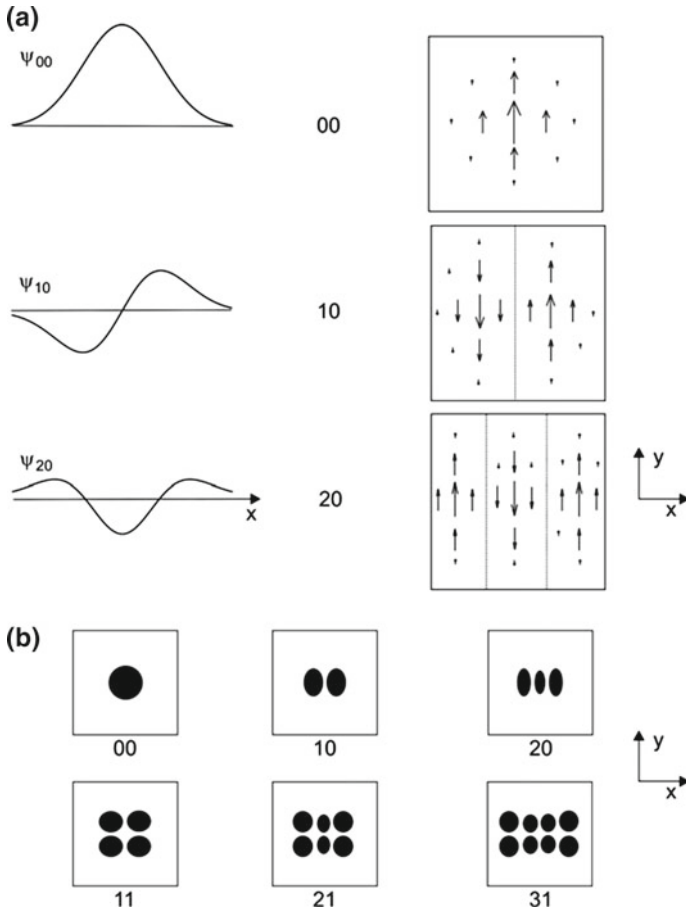


Fig. 11.10 Longitudinal and transverse modes. **a** Amplitude distributions and field lines. **b** Intensity distributions

$$\phi(z_i) = \tan^{-1} \frac{z_i - z_0}{z_R}, \tag{11.109}$$

and where $z_1=0$ and $z_2=L$. We obtain the resonance frequencies

$$\nu_{lmn} = \frac{c}{2L} \left[l + \frac{1 + m + n}{\pi} \cos^{-1}(\pm \sqrt{g_1 g_2}) \right]. \tag{11.110}$$

The frequency separations between longitudinal and transverse modes depend on the values of g_1 and g_2 . The frequency separation between two neighboring modes $mn(1 + 1)$ and mnl is always $c/(2L)$.

Figure 11.11 shows special cases that follow from (11.110).

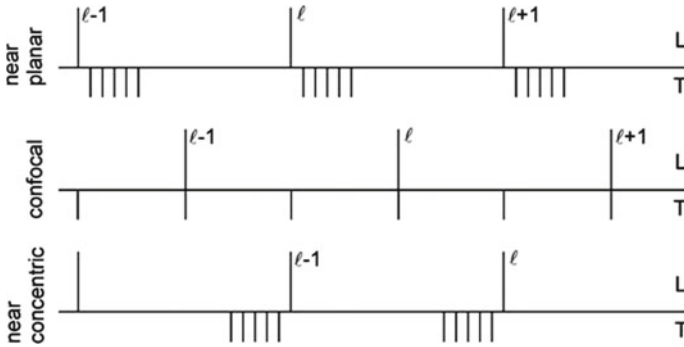


Fig. 11.11 Resonance frequencies of longitudinal (L) and transverse (T) modes

- The frequencies of the transverse modes mnl of a near-planar resonator lie near the frequency of the longitudinal mode $00l$, at slightly larger frequencies.
- A confocal resonator has a transverse mode for which the sum $m + n$ is an odd number is degenerate with an l mode, as it follows from $\cos^{-1} 0 = \pi/2$; a transverse mode for which the sum $m + n$ is an even number has a frequency between two frequencies of longitudinal modes.
- A near-concentric resonator has transverse modes mnl at frequencies slightly smaller than the frequency of the $00(l-1)$ longitudinal modes, as it follows from $\cos^{-1}(-1) = \pi$.

We note that the solution (11.106) can also be written in a form,

$$\psi_{mn}(x, y, z) = H_m\left(\sqrt{\frac{2}{F}} x\right) H_n\left(\sqrt{\frac{2}{F}} y\right) \frac{C_{3,mn}}{(ikF/2)^{1+m+n}} e^{-i[kz - (x^2+y^2)/F]}, \tag{11.111}$$

that contains the complex beam parameter $F(z)$, which is the same as for a fundamental Gaussian wave.

In our study of Gaussian waves, we have made use of Cartesian coordinates. The solution to the Helmholtz equation of paraxial waves provides the fundamental Gaussian waves and the Hermite-Gaussian waves. The number pair mn describes the variation of the sign of the amplitude along the x and the y axis. Solutions to the Helmholtz equation are Laguerre-Gaussian modes too. These are also characterized by a number pair mn , however m now describes the variation of the sign of the amplitude in radial direction and n the variation in azimuthal direction. The waves are also TEM waves. The Laguerre-Gaussian modes are obtained by solving the Helmholtz equation written in cylinder coordinates. Depending on the experimental arrangement of a laser, either type of higher-order Gaussian mode can be observed.

11.7 The Gouy Phase

The field of a Gaussian wave is given by

$$E(z, r, t) = A_0 \frac{w_0}{w} e^{-r^2/w^2} \cos(\omega t - [k(z - z_0) - \phi + kr^2/2R]). \quad (11.112)$$

A_0 is the amplitude, w_0 the beam radius in the beam waist, z_0 the position of the beam waist, $w(z)$ the beam radius at the position z , k the wave vector of the radiation, ϕ the Gouy phase and $kr^2/2R(z)$ a phase in lateral direction that is zero on the beam axis; we have chosen the phase ϕ_0 so that the beam waist lies at z_0 . The beam radius is

$$w(z) = w_0 \sqrt{1 + \frac{(z - z_0)^2}{z_R^2}}, \quad (11.113)$$

where

$$z_R = kw_0^2/2 = \pi w_0^2/\lambda \quad (11.114)$$

is the Rayleigh range. The Gouy phase (Fig. 11.12, upper part) is given by

$$\phi(z) = \tan^{-1} \frac{z - z_0}{z_R}. \quad (11.115)$$

The curvature of the wave front is

$$R(z) = z - z_0 + \frac{z_R^2}{z - z_0}. \quad (11.116)$$

The derivative of the time-dependent portion ϕ_t of the phase yields the frequency,

$$d\phi_t/dt = \omega. \quad (11.117)$$

From the position-dependent portion of the phase,

$$\phi_z = k(z - z_0) - \phi, \quad (11.118)$$

we obtain, by differentiation, the effective wave vector

$$k_{\text{eff}} = k - d\phi/dz. \quad (11.119)$$

The effective wavelength is

$$\lambda_{\text{eff}} = \frac{2\pi}{k_{\text{eff}}} = \frac{\lambda}{1 - k^{-1}d\phi/dz} = \frac{\lambda}{1 - \lambda/(2\pi)d\phi/dz}, \quad (11.120)$$

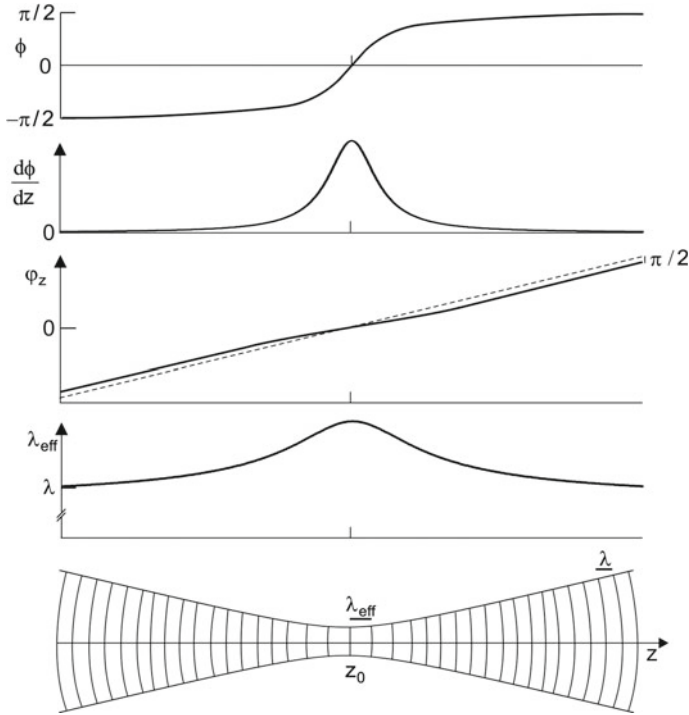


Fig. 11.12 Gaussian beam: Gouy phase; variation of the Gouy phase; spatial part (*dashed*) of the phase and total phase (*solid*); effective wavelength; wavefronts

where $\lambda=2\pi/k$ is the wavelength of the radiation far outside the beam waist. The effective wave vector and the effective wavelength depend on the position z . The Gouy phase shows the strongest change in the Rayleigh range and the derivative

$$\frac{d\phi}{dz} = \frac{1/z_R}{1 + (z - z_0)^2/z_R^2} \tag{11.121}$$

has a maximum at the center of the beam waist. We consider a wave front, which propagates through the beam waist from a far-field location z_1 to a far-field location z_2 (Fig. 11.12, third panel). The phase far outside the beam waist, at $z_1 - z_0 < 0$, is given by

$$\varphi_{(z_1)} = k \times (z_1 - z_0) + \pi/2, \tag{11.122}$$

and for the range far outside the beam waist at $z_2 - z_0 > 0$ by

$$\varphi_{(z_2)} = k \times (z_2 - z_0) - \pi/2. \tag{11.123}$$

The Gouy phase shift at a transit of radiation through the beam waist, from a far-field location to a location in the other far-field is equal to $-\pi$. In the range of the beam waist, the effective wavelength (Fig. 11.12, lower panels) is larger than λ . In the center of the beam waist, the effective wavelength is equal to $\lambda_{\text{eff}} = \lambda + \lambda/(4\pi)$. The wave fronts have the largest distance in the center of the beam waist. The sum of all differences $\lambda_{\text{eff}} - \lambda$ at a transit of radiation through the beam waist is equal to $\lambda/2$.

We now discuss the Gouy phase shift of radiation in a resonator. The field of a standing wave of an open resonator is

$$E(z, r, t) = A_0 \frac{w_0}{w} e^{-r^2/w^2} \cos[k(z - z_0) - \phi + kr^2/2R] \cos \omega t. \quad (11.124)$$

The resonance condition requires that

$$2kL - \Delta\phi = l \times 2\pi; \quad l = 1, 2, \dots, \quad (11.125)$$

where l is the order of resonance and $\Delta\phi$ the Gouy phase shift per round trip. At resonance, the phase change $2kL$ per round trip transit is larger than 2π because of the Gouy phase shift,

$$2kL = l \times 2\pi + \Delta\phi. \quad (11.126)$$

It follows that the resonance frequencies are

$$\nu_l = l \times \frac{c}{2L} + \nu_{\text{Gouy}}, \quad (11.127)$$

where ν_{Gouy} is the *Gouy frequency*,

$$\nu_{\text{Gouy}} = \frac{\Delta\phi}{2\pi} \times \frac{c}{2L}. \quad (11.128)$$

The resonance frequencies of an open resonator (Fig. 11.13) are multiples of $c/2L$ but shifted toward higher frequencies by the Gouy frequency.

Figure 11.14 and Table 11.3 show values of Gouy frequencies of stable resonators. The Gouy frequency is zero for a Fabry–Perot resonator and has the largest value

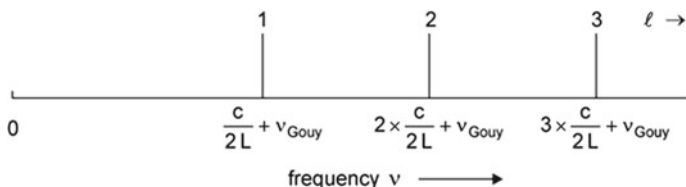


Fig. 11.13 Low-order resonance frequencies of an open resonator

Fig. 11.14 Gouy frequency of a stable resonators

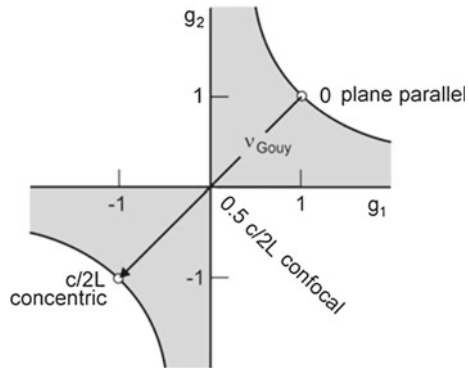


Table 11.3 Gouy phase shift and Gouy frequency of resonators

Resonator	$\Delta\phi$	ν_{Gouy}
Fabry-Perot	0	0
Symmetric confocal	π	$0.5 c/(2L)$
Semiconfocal	$\pi/2$	$0.25 c/(2L)$
Symmetric concentric	2π	$c/(2L)$

for a concentric resonator. The Gouy frequency of a symmetric confocal resonator is $\nu_{\text{Gouy}} = (1/2)c/2L$.

Example The Gouy phase shift of a symmetric confocal resonator of a length of 0.5 m is $\Delta\phi = \pi$ and the Gouy frequency is $0.5c/(2L) = 150 \text{ MHz}$; for a semiconfocal resonator of the same length, the Gouy phase shift is $\pi/2$ and the Gouy frequency is 75 MHz.

In 1891, Louis Gouy (Lyon, France) found that an electromagnetic wave changes the phase by π if it propagates through a focus point—besides the phase change due to spatial propagation [70–72]. Gouy studied an interference pattern of two beams (arising from the same white light source), which were reflected from two plane mirrors, and observed an additional phase shift when he replaced one of the mirrors by a spherical mirror that produced a focus point in one of the beams; Gouy derived the phase shift from an analysis of the focusing process by use of Huygens’ principle. Various studies in the years shortly after 1900 confirmed the results (*see* [73]).

The Gouy phase shift has also been observed by means of coherent waves—waves with well-defined amplitudes and phases. Experiments have been performed with microwaves [74], near infrared radiation [75] and far infrared radiation [76]. We describe the far infrared experiment (Fig. 11.15). The radiation consisted of single-cycle terahertz radiation wave packet, generated with a small-area source. The radiation was made parallel with a lens and focused with another lens to a small-area detector. The detector monitored the time dependent amplitude and phase of the radiation at the position of the detector. Alternatively, two additional lenses produced

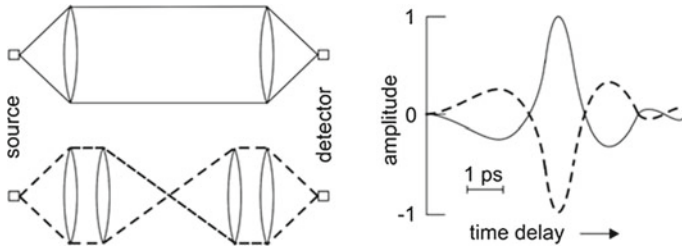


Fig. 11.15 Measurement of the Gouy phase shift

a focus point between source and detector. Signals were measured at different time delays relative to the starting time of a pulse. The experiment showed that the phase of a wave packet changed by π when the wave propagated through the focus; we will describe the method of measuring phases and amplitudes of electromagnetic fields in Sect. 13.5.

We can ask: is the group velocity of radiation traversing a beam waist smaller than the speed of light? The answer is no: the change of phase by π causes a reversal of the direction of the electric field of the wave. The group velocity remains therefore unchanged.

11.8 Diffraction Loss

Up to now, we have neglected loss by diffraction at the resonator mirrors. The diffraction loss depends on the resonator type. Figure 11.16 shows examples of the diffraction loss δ (=loss per round trip) for resonators of different Fresnel numbers (F).

- The diffraction loss of radiation in a confocal resonator is (for $F \geq 0.5$) much smaller than the diffraction loss of radiation in a planar resonator.
- Longitudinal modes have a smaller diffraction loss than transverse modes.
- The diffraction loss decreases strongly with increasing Fresnel number.

The theory of Kirchhoff (1882) allows for determination of diffraction loss. We give here a short sketch of the theory. We are looking for a solution of the wave equation in the form of the Helmholtz equation,

$$\nabla^2 \psi + k^2 \psi = 0. \tag{11.129}$$

Originally, Kirchhoff formulated the theory assuming that a parallel light wave is incident on an iris diaphragm (Fig. 11.17a). The boundary condition is the following: in the open part of the iris, the field has the same value ψ as without iris. According to Huygens' principle, spherical waves are leaving from each point in the open part of

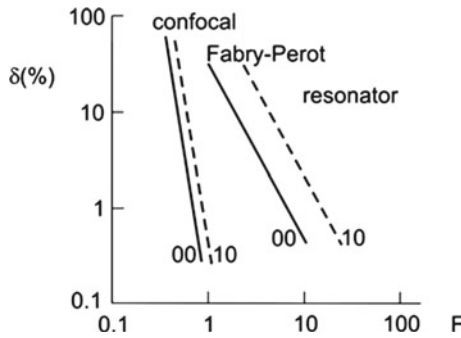


Fig. 11.16 Diffraction loss per round trip

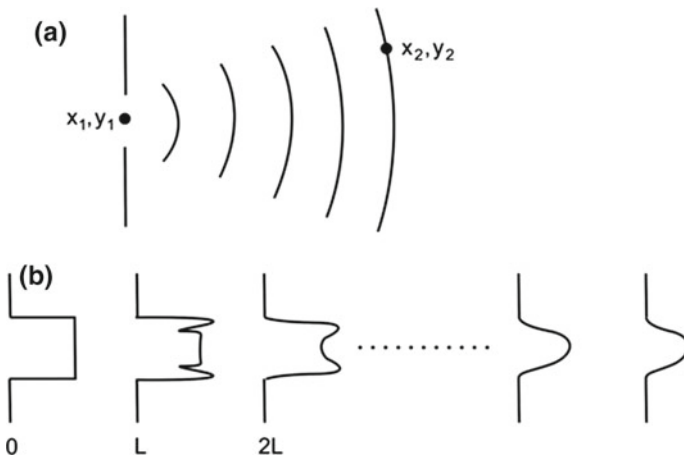


Fig. 11.17 Diffraction. **a** Diffraction at an iris diaphragm. **b** Multiple diffraction at iris diaphragms in series

the iris. The field amplitude at a point (x_2, y_2) is the sum of all partial waves arriving from all points x_1, y_1 in the open part of the iris. The summation yields

$$\psi(x_2, y_2) = \frac{ik}{4\pi} \int (1 + \cos \theta) \frac{e^{iks}}{s} \psi(x_1, y_1) dx_1 dy_1. \tag{11.130}$$

The amplitude depends on the distance s between the iris and the point (x_2, y_2) and on the angle θ between the central axis and the direction between the iris and the point; s is large compared to the diameter of the open part of the iris. The solution obeys the Helmholtz equation. The factor i to the integral (11.130) implies the occurrence of the Gouy phase shift.

Radiation in a resonator undergoes *multiple reflection with diffraction*, illustrated in Fig. 11.17b for iris diaphragms in series. The calculation starts with an arbitrarily assumed field distribution $\psi_1(x_1, x_2)$, for instance, a constant distribution over one

of the mirrors. A first integration provides the distribution at the second mirror—at a single transit through the resonator. The numerical calculation of ψ_{n+1} from ψ_n , where n is the number of passes through the resonator, leads to the following results.

- *Stable resonator.* After a field has performed a certain number of transits through the resonator, the field obeys the relation

$$\psi_{n+1}(x, y) = \eta \psi_n(x, y), \tag{11.131}$$

where $\eta (< 1)$ is a number. The shape of the field distribution is reproduced, but there is a loss at each reflection.

- *Unstable resonator.* The distribution $\psi(x, y)$ does not stabilize.

We have seen that in the far field of a fundamental Gaussian wave the product of the beam diameter and the angle of aperture is a constant,

$$D_0 \times \theta_0 = \frac{4}{\pi} \lambda. \tag{11.132}$$

$D_0=2w_0$ is the diameter of the field distribution at the beam waist. If diffraction at the output coupling mirror or at another optical element in a laser resonator enhances the angle of aperture, the beam diameter D can be larger than D_0 and the angle θ can be larger than θ_0 . The product can be written as

$$D \times \theta = M^2 D_0 \theta_0. \tag{11.133}$$

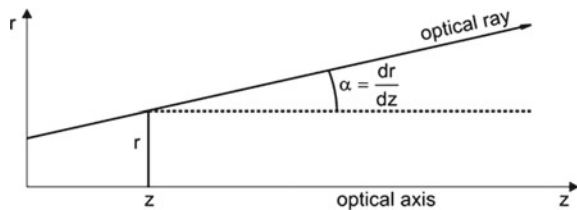
The M factor is a measure of the quality of a beam. $M = 1$ corresponds to a Gaussian beam.

11.9 Ray Optics

We characterize an optical ray (Fig. 11.18) at a the point z, r by the vector

$$\mathbf{r} = \begin{pmatrix} r \\ r' \end{pmatrix}, \tag{11.134}$$

Fig. 11.18 Paraxial optical beam



where r is the distance of the ray from the beam axis and $r' = dr/dz$ is the slope of the ray. The slope of a paraxial ray is approximately equal to the angle between the ray and the optical axis. Therefore, we can make use of the approximation $dr/dz = \sin \alpha \approx \alpha$.

We describe the trajectory of an optical ray propagating from a location r_1 to a location r_2 by

$$r_2 = \begin{pmatrix} A & B \\ C & D \end{pmatrix} r_1, \tag{11.135}$$

where $\begin{pmatrix} A & B \\ C & D \end{pmatrix}$ is the *ray matrix* (=ABCD matrix).

The propagation of an optical ray in an optical system with s optical elements in series is described by the matrix product

$$\begin{pmatrix} A & B \\ C & D \end{pmatrix} = \begin{pmatrix} A_s & B_s \\ C_s & D_s \end{pmatrix} \cdots \begin{pmatrix} A_2 & B_2 \\ C_2 & D_2 \end{pmatrix} \begin{pmatrix} A_1 & B_1 \\ C_1 & D_1 \end{pmatrix}. \tag{11.136}$$

We illustrate the method by various examples (Fig. 11.19).

- *Propagation in free space*; $\begin{pmatrix} A & B \\ C & D \end{pmatrix} = \begin{pmatrix} 1 & L \\ 0 & 1 \end{pmatrix}$.

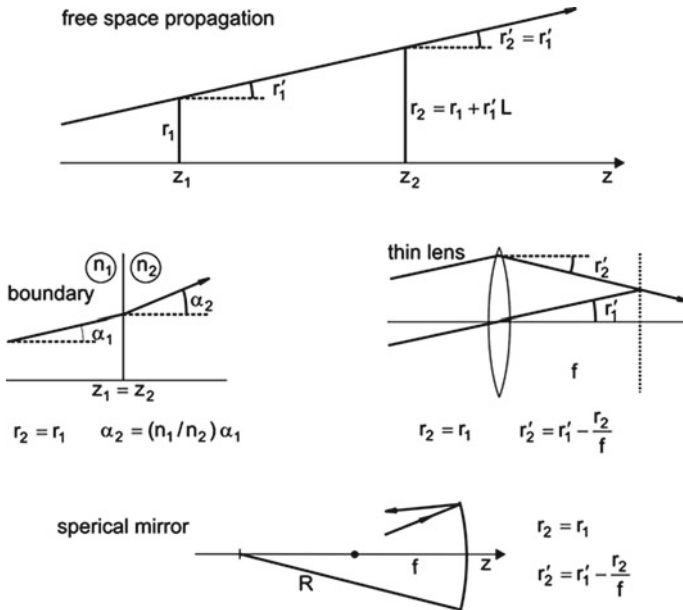


Fig. 11.19 Optical rays in different systems

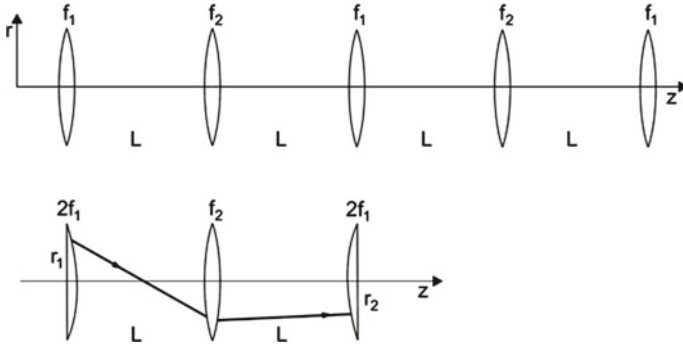


Fig. 11.20 Optical beam passing lenses in series (*upper part*) and periodicity interval (*lower part*)

- Snell's law; $\begin{pmatrix} A & B \\ C & D \end{pmatrix} = \begin{pmatrix} 1 & 0 \\ 0 & n_1/n_2 \end{pmatrix}$.
- Thin lens with a focus length f ; $\begin{pmatrix} A & B \\ C & D \end{pmatrix} = \begin{pmatrix} 1 & 0 \\ -f^{-1} & 1 \end{pmatrix}$.
- Spherical mirror; $\begin{pmatrix} A & B \\ C & D \end{pmatrix} = \begin{pmatrix} 1 & 0 \\ -2R^{-1} & 1 \end{pmatrix} = \begin{pmatrix} 1 & 0 \\ f^{-1} & 1 \end{pmatrix}$. The radius has a positive sign ($R > 0$) for a concave mirror and a negative sign ($R < 0$) for a convex mirror.

We derive, by the use of ray optics, the stability criterion for resonators. A spherical mirror and a thin lens are equivalent optical elements. Accordingly, we can replace a two-mirror resonator by a series of lenses with the focus lengths $f_1=R_1/2$ and $f_2=R_2/2$ (Fig. 11.20). The periodicity interval of the series of lenses includes a half-lens with the focus length $2f_1=R_1$, a lens with the focus length $f_2 = R_2/2$ and another half lens with the focus length $2f_1 = R_1$. A round trip through the resonator corresponds to the path through the periodicity interval in the lens system from r_1 to r_2 , where

$$r_2 = \begin{pmatrix} 1 & 0 \\ -(2f_1)^{-1} & 1 \end{pmatrix} \begin{pmatrix} 1 & L \\ 0 & 1 \end{pmatrix} \begin{pmatrix} 1 & 0 \\ -f_2^{-2} & 1 \end{pmatrix} \begin{pmatrix} 1 & L \\ 0 & 1 \end{pmatrix} \begin{pmatrix} 1 & 0 \\ -(2f_1)^{-1} & 1 \end{pmatrix} r_1. \quad (11.137)$$

We obtain, with the mirror parameters $g_1 = 1 - L/R_1$ and $g_2 = 1 - L/R_2$, the ABCD matrix

$$r_2 = \begin{pmatrix} 2g_1g_2 - 1 & 2g_2L \\ -2g_1(g_1g_2 - 1)L^{-1} & 2g_1g_2 - 1 \end{pmatrix} r_1. \quad (11.138)$$

We are looking for rays that remain unchanged after the propagation through a periodicity interval. A stable trajectory requires that

$$\begin{pmatrix} A & B \\ C & D \end{pmatrix} r_1 = \eta r_1 \quad (11.139)$$

and $|\eta| = 1$. The eigenvalue equation

$$\begin{pmatrix} A - \eta & B \\ C & D - \eta \end{pmatrix} \begin{pmatrix} r_1 \\ r'_1 \end{pmatrix} = 0 \quad (11.140)$$

leads to

$$\begin{vmatrix} A - \eta & B \\ C & D - \eta \end{vmatrix} = 0, \quad (11.141)$$

$$\eta^2 - 2(2g_1g_2 - 1)\eta + 1 = 0, \quad (11.142)$$

$$\eta_{a,b} = 2g_1g_2 - 1 \pm \sqrt{(2g_1g_2 - 1)^2 - 1}. \quad (11.143)$$

There are two possibilities.

- η_a and η_b are real if $g_1g_2 \geq 1$. This corresponds to instable resonators because, after N round trip transits through the resonator and $N \rightarrow \infty$, the vector

$$\begin{pmatrix} r_N \\ r'_N \end{pmatrix} = \eta^N \begin{pmatrix} r_1 \\ r'_1 \end{pmatrix} \quad (11.144)$$

diverges.

- η_a and η_b are imaginary if $g_1g_2 < 1$. This is the stability criterion. We obtain $\eta_{a,b} = \exp(\pm i\varphi)$, where $\cos \varphi = 2g_1g_2 - 1$. After N round trip transits, the vectors

$$\begin{pmatrix} r_N \\ r'_N \end{pmatrix} < |\eta_{a,b}| e^{\pm i\varphi} \begin{pmatrix} r_1 \\ r'_1 \end{pmatrix} \quad (11.145)$$

remain stable because $|\eta_a| = |\eta_b| < 1$. In our derivation of the stability criterion, we did not specify the values of r_1 and r'_1 . Thus, the result is valid for all paraxial rays.

It is possible to describe the propagation of a Gaussian beam through an optical system by the use of the ABCD matrix of the optical system. We have found, *see* (11.41) and (11.42), that a Gaussian beam can be characterized by the complex beam parameter $\tilde{q}(z)$. We now make use of this complex beam parameter: if the complex beam parameter $\tilde{q}_1(z_1)$ is known, then $\tilde{q}_2(z_2)$ follows from the relation

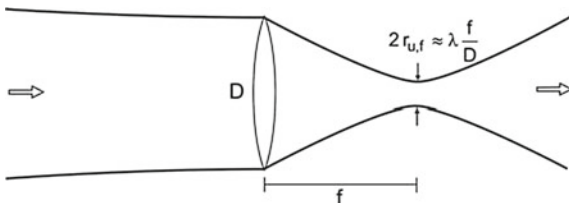
$$\tilde{q}_2 = \frac{A\tilde{q}_1 + B}{C\tilde{q}_1 + D} \quad (11.146)$$

or

$$\frac{1}{\tilde{q}_2} = \frac{C + D/\tilde{q}_1}{A + B/\tilde{q}_1} = \frac{1}{R(z_2)} - \frac{i\lambda}{\pi w^2(z)}. \quad (11.147)$$

We mention two examples.

Fig. 11.21 Focusing of a Gaussian beam by a lens



Example propagation of a Gaussian beam from the location z_0 (beam waist) to a location z . The elements of the ABCD matrix for propagation in free space are $A = 1$, $B = z - z_0$, $C = 0$, and $D = 1$. At the beam waist, we have $R(z_0) = \infty$, $w(z_0) = w_0$, and $1/\tilde{q}_1 = -i\lambda/\pi w_0^2$. It follows, for $z = z_2$, that

$$\frac{-i\lambda(\pi w_0^2)^{-1}}{1 - i\lambda(\pi w_0^2)^{-1}(z - z_0)} = \frac{1}{R(z)} - \frac{i\lambda}{\pi w^2(z)}. \tag{11.148}$$

Equating real and imaginary parts leads to expressions for $w(z)$ and $R(z)$ that we derived (in Sect. 11.3) by the use of the Helmholtz equations; see (11.24) and (11.25). The agreement may be seen as a justification of the relation (11.146).

Example focusing a Gaussian beam by a thin lens (Fig. 11.21). A thin lens is located in the beam waist of a Gaussian beam. The ABCD matrix describing propagation through a thin lens at z_0 and then over a distance $z - z_0$ is

$$\begin{pmatrix} A & B \\ C & D \end{pmatrix} = \begin{pmatrix} 1 & z - z_0 \\ 0 & 1 \end{pmatrix} \begin{pmatrix} 1 & 0 \\ -f^{-1} & 1 \end{pmatrix} = \begin{pmatrix} 1 - (z - z_0)f^{-1} & z \\ -f^{-1} & 1 \end{pmatrix}. \tag{11.149}$$

We find, with $1/\tilde{q}_1 = -i/z_R = -i\lambda/(\pi w_0^2)$ and

$$\frac{-f^{-1} - iz_R^{-1}}{1 - (z - z_0)f^{-1} - i(z - z_0)z_R^{-1}} = \frac{1}{R(z)} - i\frac{\lambda}{\pi w^2(z)}, \tag{11.150}$$

the values

$$\frac{1}{R(z)} = \frac{-f^{-1} + (z - z_0)(f^{-2} + z_R^{-2})}{1 - (z - z_0)^2 f^{-2} + (z - z_0)^2 z_R^{-2}}, \tag{11.151}$$

$$\frac{\lambda}{\pi w^2(z)} = \frac{z_R^{-1}}{(1 - (z - z_0)^2 f^{-2} + (z - z_0)^2 z_R^{-2})}. \tag{11.152}$$

At the focus point of the lens, $z = z_f$, the curvature $R(z_f)$ is infinitely large. It follows that

$$z_f - z_0 = \frac{f}{1 + f^2 z_R^{-2}} \tag{11.153}$$

or, for $f \ll z_R$, that $z_f - z_0 \approx f$. The radius of the beam in the focus of the lens is

$$w_f = \frac{\lambda f}{\pi w_0}. \quad (11.154)$$

With respect to the energy distribution, the beam radius is $r_{u,f} = w_f/\sqrt{2}$ and the angle of divergence is $\Theta_{u,f} = w_0/(f\sqrt{2})$. The radiance in the focus of the lens,

$$L_u = \frac{P}{\pi^2 r_{u,f}^2 \theta_{u,f}^2}, \quad (11.155)$$

is the same as in the incident Gaussian beam, namely $P/(\lambda/2)^2$ in units of $\text{Wm}^{-2} \text{sr}^{-1}$. When a Gaussian beam traverses more than one optical element and all optical elements in the beam produce ideal images (without optical aberration and without diffraction), the radiance is the same at any location along the beam.

The diameter of the wave (with respect to the energy density) is

$$2r_{u,f} = \frac{\lambda}{\pi} \frac{f}{w_0}. \quad (11.156)$$

A lens of focal length $f = \pi w_0$ focuses the radiation of a Gaussian beam to an area with a diameter that is about equal to the wavelength of the radiation. If we choose a lens of diameter $D = 2w_0$, the diameter of the focused beam is equal to

$$2r_{u,f} = \frac{2\lambda}{\pi} \frac{f}{D} \sim \lambda \frac{f}{D}. \quad (11.157)$$

The beam diameter is λ , i.e., $2r_{u,f} = \lambda$, if the *f-number* of the focusing lens is $f/D = \pi/2 \sim 1.6$. It follows that a lens with an f-number of 1.6 can focus a Gaussian beam to an area $\pi(\lambda/2)^2 \approx \lambda^2$. The light intensity in the focus is

$$I_f = \frac{P}{\lambda^2}, \quad (11.158)$$

where P is the power of the radiation.

We mention another radiometric quantity, the *brilliance* of a beam:

$$B = \frac{r_p}{\Omega \Delta\nu}. \quad (11.159)$$

The brilliance of an optical beam is equal to the photon flux r_p (number of photons per second and m^2) divided by the solid angle of the beam and by the bandwidth of the radiation. For a detailed discussion of radiometric (physical) quantities and photometric quantities (how the human eye records radiation), see [29].

References [1–4, 6–11, 26, 29, 40, 64–76].

Problems

11.1 Gaussian wave.

- Determine the energy that is contained in a sheet (perpendicular to the beam axis) of thickness δz at the position z .
- Calculate the portion of power of radiation passing an area that has the beam radius $r_{u,0} = r_0$.
- Evaluate the radius r_p of the area passed by radiation of a portion p of the total power of the Gaussian wave.
- Evaluate r_p if $p = 95\%$.
- Evaluate r_p if $p = 99\%$.
- Determine the power of the radiation that passes an area of radius $r_p \ll r_0$.

11.2 Determine the minimum diameter of the tube of a helium–neon laser ($\lambda_L = 633 \text{ nm}$) that is necessary to keep, per round trip, 99% of the radiation within a confocal resonator ($L = 0.5 \text{ m}$).

11.3 Angle of divergence. Determine the angle of divergence of a Gaussian beam generated by a helium–neon laser (resonator length 0.5 m; radius of the energy density distribution at the beam waist $r_{u,0} = 0.16 \text{ mm}$; wavelength 633 nm).

11.4 Photon density in a Gaussian wave. An argon ion laser (length 1 m; radius of the beam waist 1 cm; wavelength 480 nm; power 1 Watt) emits a Gaussian wave. By the use of a telescope, the angle of aperture diminishes by a factor of 10. Estimate the number of photons arriving each second at a detector of 2 cm diameter at different distances between laser and detector.

- 100 km.
- 374,000 km (distance earth-moon).

11.5 ABCD matrix. Determine the effective focal length of an arrangement of two thin lenses (focal lengths f_1 and f_2) in contact.

11.6 Transversality of the radiation of a Gaussian wave. If a polarizer is located in a parallel beam of polarized radiation, the amplitude of the field transmitted by the polarizer is $A = A_0 \cos \theta$, where θ is the angle between the direction of polarization of the incident wave and the direction of the radiation for which the polarizer is transparent. (We assume that the transmissivity of the polarizer is 1 for $\theta = 0$.) Determine the loss of power of a Gaussian wave passing a polarizer (that is assumed to be thin compared to the Rayleigh range z_0 if the polarizer is located at different positions.

- In the beam waist at z_0 .
- At $z = z_0/2$.
- At $z = z_0$.
- At $z \gg z_0$.

- (e) Estimate the contribution of the polarizer to the V factor of a confocal laser resonator of 1 m length if the polarizer has a thickness of 1 cm and is located in the center of the resonator.

11.7 Hermite-Gaussian wave. Given is a 10l Hermite–Gaussian wave.

- (a) Determine the radius of the wave at the beam waist and the angles of divergence in the far-field.
 (b) Compare the results with corresponding values of a 00l Gaussian wave.

11.8 Calculate the Gouy phase of a Gaussian wave ($\lambda=0.6 \mu\text{m}$; $w_0 = 1 \text{ mm}$) for propagation from the center of the beam waist over a distance of one wavelength; 1 mm; 1 cm; and 1 m.

11.9 Calculate the Gouy phase per round trip transit through a resonator of a Gaussian wave ($\lambda=0.6 \mu\text{m}$).

- (a) If the resonator is a near-planar resonator with two mirrors (radius of curvature $R_1 = R_2 = 7 \text{ m}$; resonator length = 1 m).
 (b) If the resonator is a near-confocal resonator (radius of curvature $R_1 = R_2 = 1.10 \text{ m}$; resonator length = 1 m).

11.10 Show that a concentric resonator is not realizable. [*Hint*: consider the beam waist and the angle of divergence.]

11.11 Show that (11.44) is a solution of the Helmholtz equation.

11.12 Derive ray matrices for different optical arrangements.

- (a) Reflection of radiation at a plane surface of a dielectric medium.
 (b) Propagation of radiation through a thin lens.
 (c) Focusing of radiation by a spherical mirror. [*Hint*: for solutions, see Sect. 11.9.]

11.13 Show that the intensity of radiation in a Gaussian beam averaged over an optical period is $I = c \epsilon_0 A^2 \pi w_0^2 / 2$ and that

$$I(z, r) = \frac{2P}{\pi w^2(z)} e^{-2r^2/w^2(z)}, \quad (11.160)$$

where $P = 2\pi \int I(z, r) r dr$ is the power of the radiation.

11.14 Estimate radiance and brilliance of radiation of a helium-neon laser (power 10 mW; angle of divergence 1 mrad; beam waist in the laser 0.5 mm; bandwidth 1 kHz) and compare the values with those of a light bulb (electric power 10 W).

11.15 Heisenberg uncertainty principle

Show that a photon in a Gaussian beam obeys the Heisenberg uncertainty relation $\Delta y \Delta p_y \geq \hbar$, where Δy is the uncertainty of the position y and Δp_y the uncertainty of the momentum p_y of the photon. [*Hint*: Show that the full width at half maximum

of the lateral energy density in the waist is equal to $D = \sqrt{2 \ln 2} w_0$ and that the full angle of divergence, related to the full width at half maximum of the lateral energy density in the far-field, is equal to $\vartheta = (\sqrt{2 \ln 2}/\pi)\lambda/w_0$. It follows that the product is $D\vartheta = (2 \ln 2/\pi)\lambda$. Now, determine the wave vector spread, according to $\vartheta = \Delta k_y/k_x$. It follows, with $\Delta y = D$ and $\Delta p_y = \hbar\Delta k_y$, that $\Delta y\Delta p_y = (4 \ln 2) \hbar$.

11.16 Gaussian beam in a medium.

Show that a Gaussian beam in a medium with the refractive index $n (> 1)$ has a smaller divergence than in free space if the beam radius in the waist is the same.

11.17 Confined Gaussian beam.

A medium with a radial dependence of the refractive index of the form $n(r) = n_0 - a r^2$, with $a > 0$, is able to guide a wave without divergence. Show that the Helmholtz equation has the solution $\psi(z, r) = \psi_0 \exp(-r^2/w_1^2 + i \lambda z/w_1^2)$, where the beam radius w_1 is given by $w_1^2 = \lambda/(\pi\sqrt{2a})$ and where λ is the vacuum wavelength. [Hint: make use of (11.4) and (11.13), with the relation $k = n \omega/c$.]